Quantification of olivine using Fe Lα in EPMA

Ben Buse, Stuart Kearns

University of Bristol

Abstract

Quantification of first series transition metal Lα X-rays is hampered by absorption and in some cases transition probabilities (fluorescence yields) varying with chemical bonding. Compound mass absorption coefficients for Fe Lα were measured in the olivine solid-solution series (Forsterite (Mg2SiO4) to Fayalite (Fe2SiO4)) and the mass absorption coefficients for Fe Lα absorbed by Fe were calculated. The mass absorption coefficients vary systematically between Fo83 and Fo0. Using the measured mass absorption coefficients for both standard and unknown and by correcting for a systematic discrepancy, consistent with varying partial fluorescence yields, a good agreement between calculated k-ratios and measured k-ratios is achieved. The systematic variations allow quantification of unknown k-ratios. The described method of quantification requires modification of matrix correction routines to allow standards and unknowns to have different mass absorption coefficients (see Llovet et al. 2016), and to incorporate solid solution mass absorption coefficients and partial fluorescence yield corrections derived from regression of experimental data.

Keywords

Mass absorption coefficients, L-line X-rays, electron probe microanalysis, low voltage, olivine

Introduction

Quantification of first series transition metals using Lα X-rays provides the potential for high resolution analysis using low accelerating potentials (<7 kV). Quantification is, however, compromised by absorption and in some cases transition probabilities (fluorescence yields) being strongly affected by chemical bonding, with x-ray production involving partially filled 3d orbitals (Pouchou & Pichoir 1985, Fialin 1990, Fialin et al. 2001). Self-absorption is most obviously manifest in terms of peak shape changes, with the peak position shifting as the high energy side of the peak is strongly absorbed. Shifting the measured peak position cannot account for this nor can peak-area intensities which whilst accounting for peak-shape changes fail to account for changes in the magnitude of absorption as a function of electronic structure (Fialin 1990). The large analytical errors that can result in using Lα lines for first series transition metals have been documented for alloyed steels (Llovet et al. 2011; Pinard & Richter 2016), zinc minerals (Fialin 1990), Fe oxides (Remond et al. 2002) and olivine (Buse & Kearns 2011). Alternatives include calibration curves to account for the anomalous behaviour (Buse & Kearns 2011) or the use of the Ll line which does not involve the outer shell orbitals (Gopon et al. 2013, Pinard & Richter 2016, Statham & Holland 2014). The intensity of the Ll line is, however, low compared to the Lα line increasing counting statistic errors.

Strategies for overcoming anomalous absorption and transition probabilities were first proposed by Pouchou & Pichoir (1985) and have recently been developed by Llovet et al. (2016). These authors measured the mass absorption coefficients and showed that for binary alloy systems, the mass absorption coefficient (MAC) and fluorescence yield vary systematically allowing accurate quantification. Similarly Remond et al (2002) showed for the dielectric materials, FeO and Fe_2O_3, quantification was possible by removing anomalous absorption using integrated peak intensities and correcting both standard (FeO) and unknown (Fe_2O_3) for absorption using measured absorption

spectra. In this paper we apply an approach similar to Pouchou & Pichoir (1985) and Llovet et al. (2016) to olivine - the dielectric solid solution forsterite (Mg_2SiO_4) – fayalite (Fe_2SiO_4) series.

Materials and methods

Ten olivine samples representing the solid solution between forsterite and fayalite were used; five from Dabbahu, Ethiopia (Fo_{83} – Fo_{33}), fayalite rockport (Fo_0, NMNH 85276), SH-11 (Fo_{89}, Batanova et al. 2017) and three internal standards (Fo_{91} – Fo_{90} and Fo_{01}). The composition of the Dabbahu samples and the internal standards was determined by Electron probe microanalysis (EPMA) at 20kV using the Fe Kα line and are given in table 1, together with the composition of the standards. Fo_{33} was used as the standard for generating k-ratios. The olivine samples, being non-conductive, were coated with the same thickness of carbon.

Table 1 Chemical composition of olivine samples measured by EPMA operating at 20kV (Cameca SX-100, University of Bristol). Fo_{00} is fayalite rockport (NMNH 85276) and Fo_{89} is SH-11 (Batanova et al. 2017)

%Fo Wt. % FeO	91	90 9.5	89 10.5	83 16	70 27	51 40	36 49	33 51	1 67	0 67.5
MgO	49.98 ±0.26	49.19	48.54 ±0.34	43.92 ± 0.15	34.67 ± 1.29	23.44 ± 0.09	15.76 ± 0.36	14.07 ± 0.21	0.49	_
SiO2	41.27 ±0.14	40.83	40.85 ±0.21	39.83 ± 0.28	37.70 ± 0.19	34.76 ± 0.17	32.79 ± 0.12	32.65 ± 0.17	28.80	29.22
CaO	0.09 ±0.00	_	0.10 ±0.00	0.33 ± 0.01	0.32 ± 0.09	0.38 ± 0.01	0.39 ± 0.03	0.44 ± 0.04	0.10	_
MnO	0.12 ±0.00	.12	0.14 ±0.00	0.25 ± 0.02	0.47 ± 0.03	1.39 ± 0.02	2.23 ± 0.05	2.57 ± 0.05	4.09	2.14
FeO	8.41 ±0.06	9.54	10.49 ±0.06	15.88 ± 0.07	26.93 ± 0.42	40.25 ± 0.03	49.09 ± 0.26	51.09 ± 0.14	66.98	67.54

Wavescans and peak and background measurements were collected using a JEOL 8530F EPMA (University of Bristol) with a peltier-cooled cold finger to minimise carbon contamination (Buse et al. 2016). Figure 1 (a-c) shows the shift in position of the Fe Lα peak with increasing Fe content and accelerating voltage due to self absorption. Figure 1d shows the absorption curves for samples Fo_{90}, Fo_{83} and Fo_{01}, calculated by dividing their 7kV spectra by their 20 kV spectra; the 20kV spectra was first normalised to the 7kV spectra using the Fe La peak (see Remond et al. 2002 for method). The absorption edge cuts through the peak, strongly absorbing the high energy side of the peak. The MAC is therefore not constant and is dependent on spectrometer position.

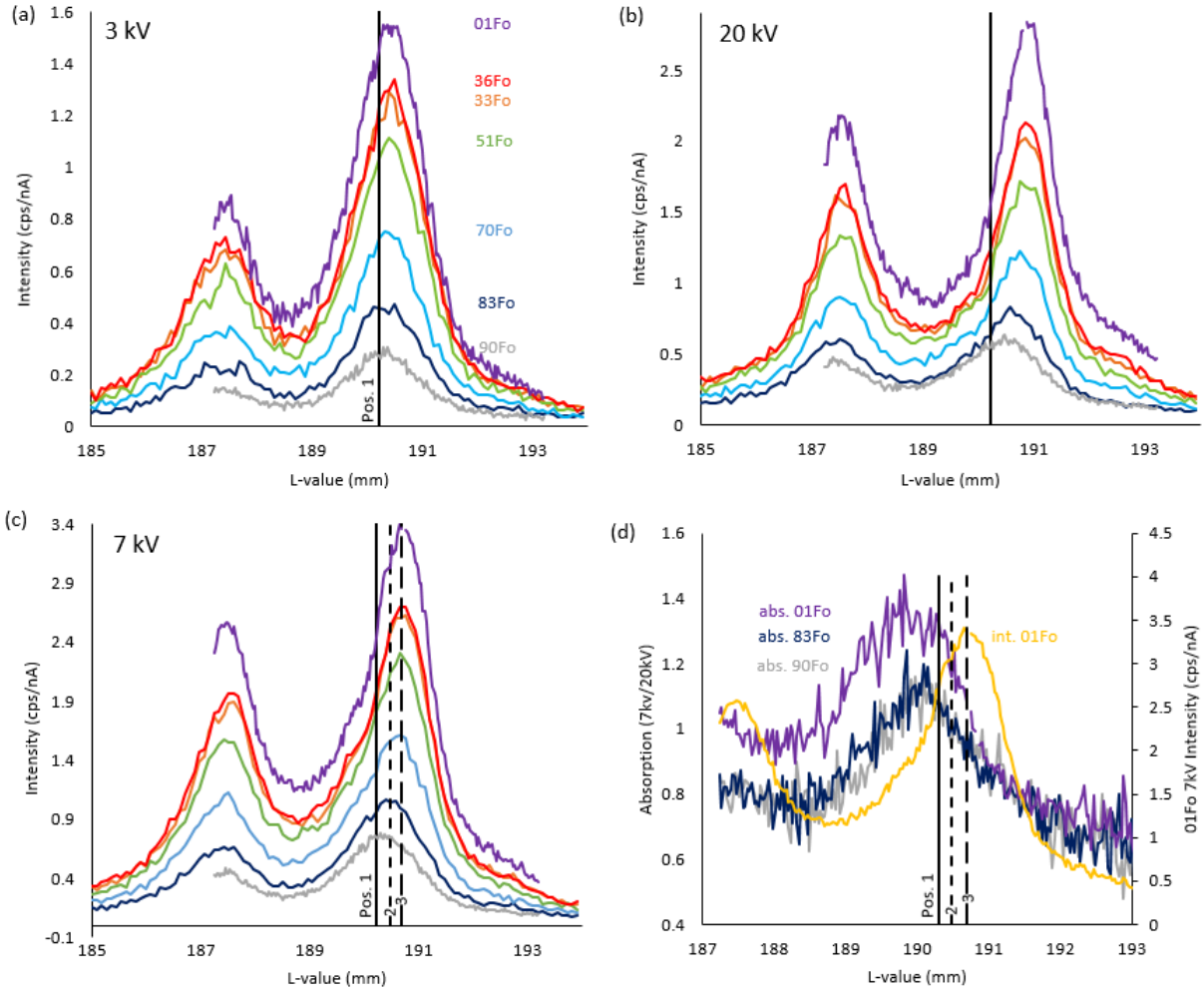

Figure 1 (a-c) Wavescans at 3kV, 7kV and 20kV for the olivine samples showing shift in the position of the Fe Lα peak with increasing Fe content and voltage due to self absorption. (d) Absorption spectra for Fo_{01}, Fo_{83} and Fo_{90} with the x-ray intensity spectra for Fo_{01} at 7kV overlain. Vertical lines give the positions at which measurements were collected.

The MAC was measured at three positions: (1) the Fe Lα peak position at 3kV for the Fo_{83} sample was selected as representing close to the true peak position because self-absorption is minimised at low accelerating voltage and low Fe content; (2) the Fe Lα peak position at 7kV for the Fo_{83} sample; (3) the Fe Lα peak position at 7kV for the Fo_{01} sample. Positions 2 and 3 were selected as representing preferential positions for 7kV analysis, at or close to the peak maximum. For each position net intensities were measured for all samples at each voltage (3, 5, 7, 10, 15 and 20 kV). Data was acquired for two different spectrometers to determine whether the measured MAC was dependant on spectrometer resolution; a spectrometer with a 140 mm Rowland circle (TAP crystal) and a spectrometer with a 100 mm Rowland circle (TAPH crystal) were used, which have FWHM wavelength resolution of 0.88 mm and 1.12 mm respectively for F in MgF_2. Count times were 60 seconds on peak and 30 seconds on each background; beam current was 140 nA.

The compound MAC, the absorption of Fe Lα by the sample, was calculated for each sample using the method of Pouchou & Pichoir (1988). Here the method was implemented using phi-rho-z curves for x-ray generation calculated using the Casino Monte Carlo package (Hovington et al. 1997). The emitted phi-rho-z curve was then calculated in Excel by correcting the phi-rho-z curve of x-ray

generation for absorption, using a specified MAC. For each depth interval the emitted phi-rho-z is given by:

$$\phi(pz)_e = \phi(pz)_g^{-(u/\rho)\rho z \operatorname{cosec}\theta}$$

where $\phi(pz)_e$ is the emitted x-ray intensity for the given depth interval, $\phi(pz)_g$ is the generated x-ray intensity for the given depth interval, (u/ρ) is the mac, ρ is the density, z is the depth, and θ is the take-off angle.

In Casino the phi-rho-z curves are normalised, therefore the modelled emitted intensity is obtained by:

$$I_e = (\int \phi(pz)_e / \int \phi(pz)_g) * I_g$$

Where I_e is the emitted intensity, $\int \phi(pz)_e$ is the integrated emitted phi-rho-z curve, $\int \phi(pz)_g$ is the integrated generated phi-rho-z curve and Ig is the generated intensity. The measured intensities were corrected for the presence of a carbon coat by calculating the intensities without absorption and energy loss from the coating using the PAP model in GMRFILM (Waldo 1988). To calculate the MAC, corrected measured intensities and modelled emitted intensities were expressed relative to 3kV, permitting comparison between modelled and measured intensities. The specified MAC was then adjusted as a free variable to minimise the discrepancy between the modelled and measured relative intensities (e.g. Figure 2). This was performed in Microsoft Excel using the solver function, which adjusts one variable to optimise another. Figure 2b shows the method applied to Pouchou and Pichoir (1985) data; the calculated MAC of 3368 cm^2/g is in close agreement to 3300 cm^2/g calculated by the authors.

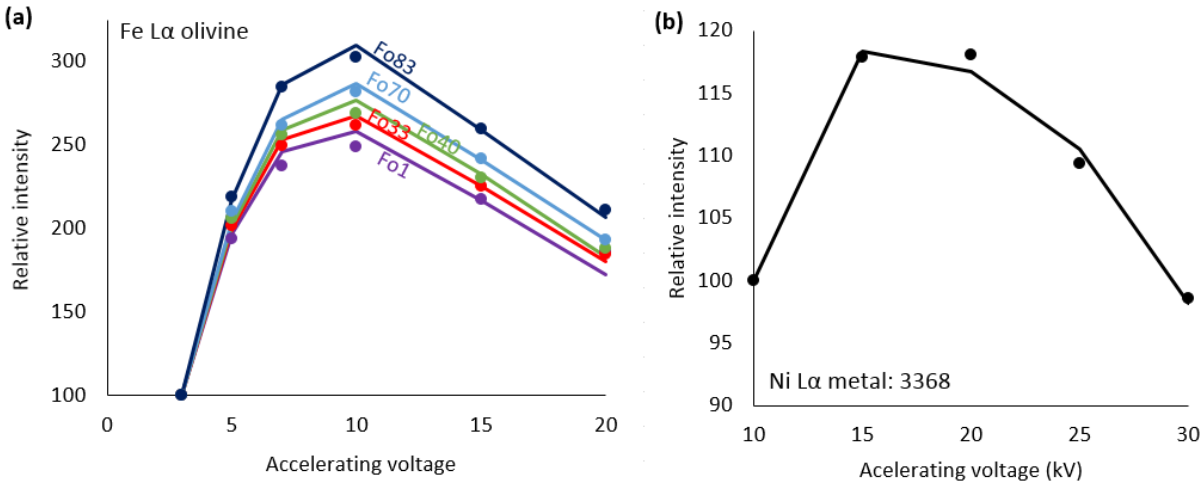

Figure 2. (a) Calculating MAC for olivine samples. (b) MAC calculated for Pouchou and Pichoir (1985) data for Ni Lα in Ni metal.

The, elemental MAC, absorption of Fe Lα by Fe, was calculated from the compound MAC by subtracting the contribution to the compound MAC from the other elements present (O, Si, Mg, Ca and Mn), using their MACs from the FFAST database. The Fe elemental MAC for each sample is expressed as convention for 100% Fe. This allows incorporation into the matrix correction using the weight fraction of the elemental MAC.

To assess whether the measured MACs improve quantification, k-ratios were calculated from modelled emitted intensities and compared to measured k-ratios. This approach allows k-ratios to be calculated for the Casino phi-rho-z curves using the default MACs and with the measured

compound MACs. It also allows the standard (Fo_{33}) to have a different MAC from the unknown when calculating k-ratios, following the method of Llovet et al. (2016).

Results

The calculated compound MACs for Fe Lα are given in Figure 3a for both spectrometers (TAP, TAPH) at each position (position 1: peak at 3kV on Fo_{83}, position 2: peak at 7kV on Fo_{83} and position 3: peak at 7kV on Fo_{01}). The Fe self-absorption results in elevated compound MACs, where Fe becomes the principle absorber rather than oxygen. Using the known absorption of Fe Lα by O, Si, Mg, Ca and Mn (from the FFAST database), the elemental MACs for Fe Lα (see Methods section for definition) were calculated from the compound MACs and are given in Figure 3b. The elemental MACs for Fe Lα differ from that for pure Fe metal and vary across the solid solution series due to chemical bonding effects (as outlined in the introduction). The MACs, with the exception of samples with < 15 wt. % FeO, display a systematic variation across the compositional range, similar to that seen for Ni Lα MACs in NiAl alloys (Pouchou & Pichoir 1985) and NiSi alloys (Llovet et al. 2016). The measured MACs decrease from position 1 to position 3 as the analysis position is moved away from the absorption maximum, as shown by the absorption spectra (Figure 1d). Repeat analysis and comparison of TAP and TAPH show a large variation in measured MACs at position 1. This appears to relate to positioning error with the peak at 3 kV on Fo_{83} broad and low intensity (see Figure 1c). Positions 2 and 3 show a close agreement between TAP and TAPH (Figure 3 and Table 2) suggesting measured MACs are not strongly affected by spectrometer resolution. Measurements at position 3 show a close agreement with repeated analysis (see Table 2) consistent with the sharp and high intensity peak at 7kV on Fo_{01} allowing accurate peak positioning.

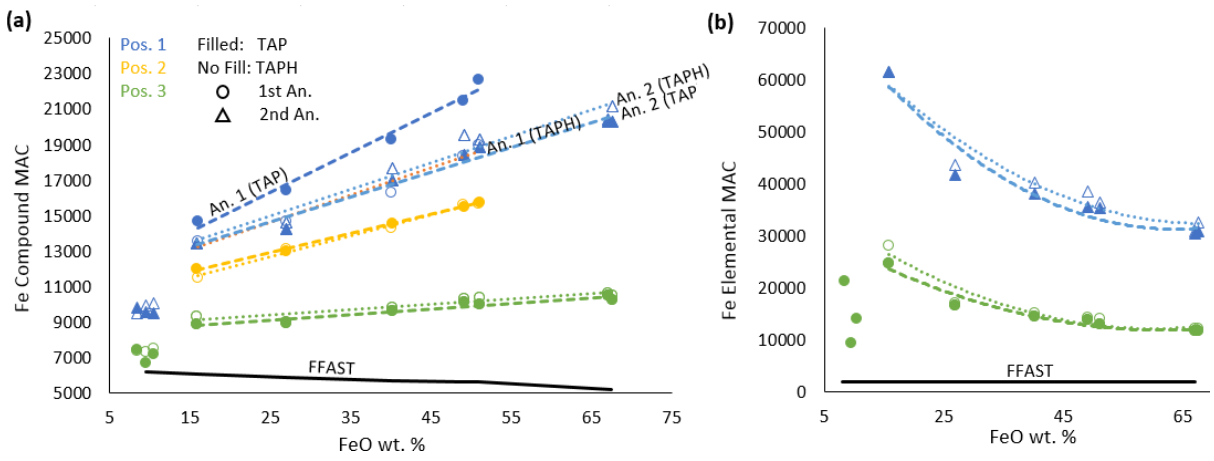

Figure 3 (a) Compound MACs for Fe Lα in the olivine samples; (b) calculated Fe elemental MAC for Fe Lα in the olivine samples.

Table 2. Variations in measured k-ratio between sessions and spectrometers (k-ratio / kratio) at 7kV

	Analysis 1/Analysis 2		TAP/TAPH	
	Pos. 1	Pos. 3	Pos. 3 An. 1	Pos. 3 An. 2
Fo0		1.00	0.98	0.98
Fo1		1.00	1.00	1.00
Fo36	1.01	1.02	0.99	1.00
Fo51	1.01	0.99	0.99	0.99
Fo70	1.03	1.01	0.98	0.99
Fo83	1.05	1.00	0.98	0.96

Fo89		1.01	0.98	0.97
Fo90		0.99	0.99	0.96
Fo91		1.00	0.97	0.96

To evaluate the improvement in quantification using the measured MACs, the calculated k-ratio is compared to the measured k-ratio. The k-ratios are shown in Figure 4 for positions 1 and 3 using Casino phi-rho-z curves. Using the Fe elemental MAC for Fe Lα from the MAC tables there is a large discrepancy between calculated k-ratio and measured k-ratio which increases with accelerating voltage (see Fo_{83}, Figure 4 a & b). This is consistent with the MAC underestimating the absorption of Fe. Using the calculated Fe elemental MACs (derived from a second-order polynomial regression of measured data – figure 3b) for both the standard and unknown, the calculated k-ratios give a good approximation to the change in measured k-ratio with voltage, but remain offset from measured k-ratios. The discrepancy between calculated and measured k-ratios (Figure 5) shows a systematic variation with composition. This is consistent with the findings of Pouchou & Pichoir (1985) and Llovet et al. (2016) who showed that this offset results from changes in the partial fluorescence yield which varies with chemical bonding effects. Using their method, and correcting for the variation in partial fluorescence yield (using a second-order polynomial regression fit to inverse average discrepancy for all voltages) the calculated k-ratios give a good agreement to the measured k-ratios (Table 3).

In Table 3 the results are shown using Casino and using Armstrong (1991) phi-rho-z equations. The spread of data is worse for Armstrong (1991) reflecting the lower coefficient of determination (r2 value) for the variation in partial fluorescence yield relative to Fo_{00}. The spread of data is also worse for position 1 than position 3 using Casino.

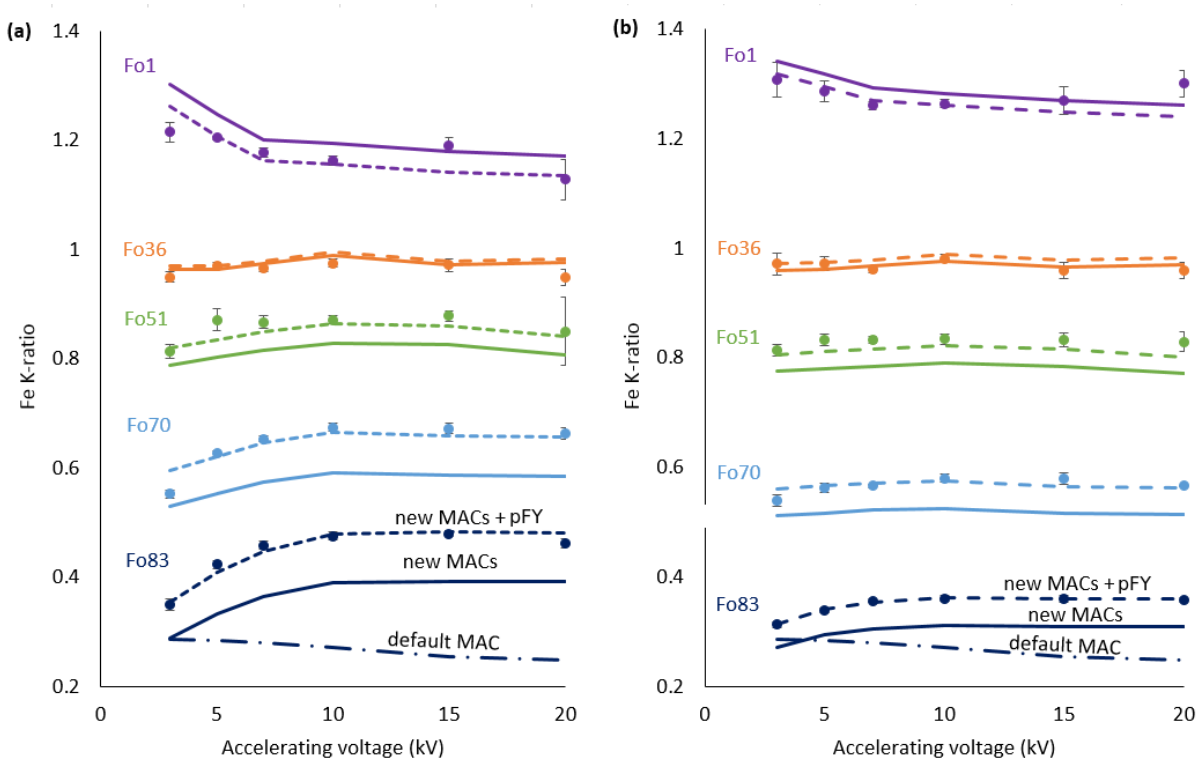

Fig 4. *Comparison of calculated Fe La k-ratios (using* I_e derived from *Casino data) and measured Fe La k-ratios for* (a) position 1, analysis 2, TAP and (b) position 3, TAP. *Error bars are 1 S.D.* Standard is Fo_{33}. pFY is correction for partial fluorescence yield.

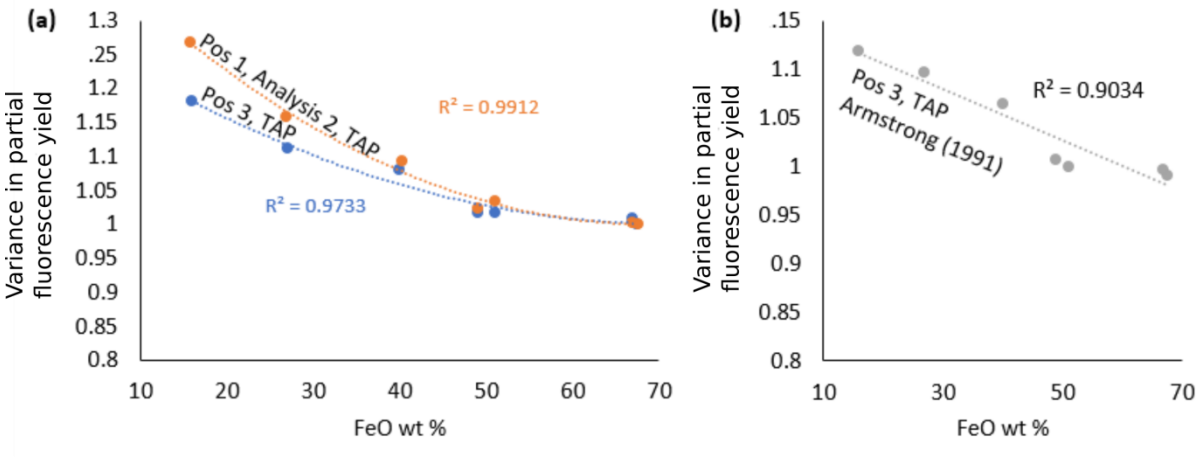

Figure 5. Variation in partial fluorescence yield relative to Fo_{00}; calculated from the inverse of the average discrepancy between calculated and measured k-ratios for all voltages. (a) calculated using Casino for positions 1 and 3. (b) calculated using Armstrong phi-rho-z (1991).

Table 3 Performance of correction procedures using measured MACs and corrected for variance in partial fluorescence yield.

		Pos. 1 TAP An.1	Pos. 1 TAP An. 2	Pos. 3 TAP	
		Casino	Casino	Casino	Armstrong (1991)
Calc. Kratio / Meas. kratio	Average	0.998	1.001	1.000	0.998
	Stdev.	2.420	2.380	1.751	2.632

Discussion

The good agreement between calculated k-ratios and measured k-ratios when using Fe elemental MACs and a correction for variance in partial fluorescence yield, both derived from second order polynomial regression demonstrate the potential for quantification of unknown compositions with > 15 wt. % Fe. To quantify unknowns, an adaptation of the current matrix correction routines is required similar to that suggested in Llovet et al. (2016) and Fialin (1990). In this approach the constant Fe elemental MAC of the matrix correction is replaced by a "solid-solution" MAC determined experimentally from regression. The standard and unknown must have separate Fe elemental MACs. In addition to a correction for Z, A and F a correction for partial fluorescence yield (pFY) is required. This is also derived experimentally from regression for the solid-solution series. The correction factor pFY is given by:

$$pFY = pFY_{Std} / pEY_{Unk}$$

where EY_{Std} and EY_{Unk} are given by the variance in partial fluorescence yield relative to Fo_{00} (Figure 5) calculated from regression for the standard and unknown respectively.

Using this modified matrix correction the k-ratios were quantified using the Armstrong (1991) phi-rho-z equations and the results are given in Table 4. As noted above, the agreement between calculated and measured k-ratios was optimum for Casino data (Table 3), suggesting errors when

calculating with Armstrong (1991) phi-rho-z could be reduced by using the same model to calculate MACs.

Table 4 Calculated compositions using measured MACs and correction for partial fluorescence yields, using Armstrong (1991)

FeO wt. %	Actual (20kV, Fe Ka)	Measured (7kV, Fe La)	Difference	Partial fluorescence yield correction
Fo83	15.88	16.36	1.030	0.900
Fo70	26.93	27.60	1.025	0.938
Fo51	40.25	41.93	1.042	0.978
Fo36	49.09	48.94	0.997	0.996
Fo1	66.98	67.38	1.006	1.028
Fo0	67.54	69.23	1.025	1.030

The method involves measurements on flank positions (Figure 1 a-c) which are more sensitive to spectrometer reproducibility. Even where positions 2 or 3 are used for 7kV analysis, shifts in the peak position with Fe concentration prevent measurement at the peak maximum for the entire compositional range. To test the contribution to analytical error repeat measurements were made over many hours. Table 5 demonstrates that at least over this time frame the error is small (< 2% relative) with the spectrometers capable of producing consistent data.

Table 5. K-ratio stability during analysis. 7kV Fo 70.

	Pos. 1 An. 2 TAP				**Pos. 3 An. 2 TAP**		
	Kratio	StdDev%	**Kratio/Initial Kratio**		**Kratio**	**StdDev%**	**Kratio/Initial Kratio**
0	0.653	0.53	1.00	0	0.570	0.77	1.00
+4hrs 5 min	0.657	0.63	1.01	+40min	0.572	0.41	1.00
56 points	0.660	0.98	1.01	52 points	0.568	1.32	1.00
+ 7hr 45 min	0.665	0.42	1.02	+4 hr	0.559	0.09	0.98

The recommended position for analysis is position 3, away from the absorption maximum. The use of the Fo_{01} peak position minimises positioning error. Position 3 also reduces the slope in MAC across the compositional range, thereby reducing the difference in Fe elemental MAC between standard and unknown. This reduces the contribution of any error in the MAC value on the calculated k-ratio and may explain the improvements in calculated k-ratios when using position 3 compared to position 1 (Table 3).

The results suggest a small effect of spectrometer resolution with k-ratios for TAPH being 1-2% relative lower than TAP (Table 2) and are within the errors of the method. To optimise quantification it may be necessary to select the MACs and partial fluorescence yield correction based upon spectrometer resolution. A binary choice between TAP or TAPH resolution may be sufficient.

The reason for the different behaviour of olivine with forserite content > 85 is unclear, with the absorption spectra for Fo90 and Fo83 being indistinguishable (Figure 1d).

The forsterite-fayalite solid solution is relatively simple and does not involve significant variations in Fe oxidation state. The applicability of this method to more complex systems in which Fe oxidation state varies is unclear for changes in Fe oxidation state have also be shown to shift peak position (Fialin et al. 2001). The MAC may vary both with composition and oxidation state. In cases where Fe oxidation state varies stoichiometrically with composition such as garnets (Hofer & Brey 2007) it should be possible to calculate solid solution MACs. This would not be possible where oxidation state varies independently of composition such as in volcanic glass.

Conclusions

Measured compound MACs and calculated Fe elemental MACs for absorption of Fe Lα in the forsterite-fayalite series show a systematic variation between Fo83 and Fo0. Using a regression fit to the calculated Fe elemental MACs for Fe Lα the change in measured k-ratio with voltage can be accurately calculated; the calculated k-ratios, however, remain offset from measured k-ratios (Figure 4). The discrepancy between calculated k-ratios and measured k-ratios is systematic between Fo83 and Fo0 and consistent with varying partial fluorescence yields (Pouchou & Pichoir (1985), Llovet et al. 2016). Once the partial fluorescence yield is accounted for, a good agreement between measured and calculated k-ratios is obtained (see Figure 4 & Table 3).

The data presented provides the potential for quantification of olivine using the Fe Lα line, allowing high spatial resolution analysis and high intensities, relative to the Ll, to be utilized. As demonstrated using the Armstrong (1991) phi rho z equations, for this potential to be realised, matrix correction routines need to be modified to (1) allow standards and unknowns to have different MACs; (2) allow the incorporation of "solid-solution" elemental MACs, calculated from regression of experimental data; (3) the incorporation of a correction for partial fluorescence yields for solid solutions calculated from regression. This is similar to the quantification of the Ni Lα signal in NiAl and NiSi alloys (Pouchou & Pichoir (1985), Llovet et al. 2016).

There are several potential sources of error to this technique: (1) spectrometer drift, this is minimal over many hours (< 2 % relative), but given the measurement on flank position should be checked from day to day; (2) the spectrometer resolution, a large change in resolution from 100 mm to 140 mm Rowland circle appears to give a systematic change of 1-2% relative; (3) optimisation of casino derived MACs to matrix models, the deviation on results using casino is 1.75 % relative compared to 2.6 % relative for Armstrong (1991) phi-rho-z equations. Further work is required to evaluate whether the method can be used for any spectrometer, but the choice of position 3 has been found to work well with the spectrometers and TAP crystals investigated.

The results show that, provided varying MACs and partial fluorescence yields are accounted for, the La line can be used with the benefit of higher intensity compared to the other L lines. However, the collection of MAC and fluorescence yield data is not trivial and care is required to avoid systematic errors. The quantification of the Ll line (Gopon et al 2013) is, by comparison, straight forward and is largely unaffected by the chemical environment providing an attractive prospect where the concentrations are sufficient to give acceptable errors.

The method outlined in this paper should be applicable to the quantification of first series transition metal Lα X-rays in other minerals provided the metal oxidation state either remains constant or varies stoichiometrically with composition.

Acknowledgements

The authors would like to thank Lorraine Field (British Geological Survey) for providing Dabbahu olivine samples for this study from her PhD thesis and Smithsonian Institution, Department of Mineral Sciences, for providing the fayalite standard (NMNH85276). The authors would like to thank Mike Matthews for reading and commenting on the manuscript prior to submission and the reviewer for helpful comments.

References

Armstrong (1991). In Electron Probe Quantitation (eds Heinrich K.F.J. & Newbury D.E.)

Batanova V, Sobolev A, Thompson J, Danyushevsky L, Goemann K, Portnyagin M, Garbe_Schoenberg D, Hauri E, Kimura J-I, Chang Q, Senda R, Chauvel C, Campillo S & Ionov D (2017). Preliminary Data on New Olivine Reference Material MongOL Sh11-2 for in situ Microanalysis. Goldschmidt conference abstract

Fialin, M. (1990). Some Considerations on the Use of Lα Series of Transition Metals in Electron Probe Microanalysis: the Example of Zinc Minerals.

Fialin, M., Wagner, C., Metrich, N., Humler, E., Galoisy, L. & Bezos, A. (2001). Fe3+/ΣFe vs. FeLα peak energy for minerals and glasses: Recent advances with the electron microprobe. *Am Min* **86** 456-465

Gopon, P., Fournelle, J., Sobol, P.E. & Llovet, X. (2013). Low-Voltage electron probe microanalysis of Fe-Si compounds using soft x-rays. *Microsc. Microanal.* **19** 1698-1708

Hofer, H.E. & Brey, G.P. (2007). The iron oxidation state of garnet by electron microprobe: Its determination with the flank method combined with major-element analysis. *Am Min* **92** 873-885

Hovington, P. Drouin, D. & Gauvin, R. (1997). CASINO: A new monte carlo code in C language for electron beam interaction – part 1: Description of the program. *Scanning* **19** 1-19

Llovet, X., Pinard, P.T., Heikinheimo, E., Louhenkilpi, S. & Richter, S. (2016). Electron Probe Microanalysis of Ni Silicides using Ni-L X-ray Lines. *Microsc. Microanal* **6** 1233-1243

Pinard, P.T. & Richter, S. (2016). Quantification of low concentration elements using soft X-rays at high spatial resolution. *IOP Conf Series Mat Sci Eng* **109** 012013

Pouchou, J.L. & Pichoir, F. (1985). Anomalies d'emission et d'absorption du rayonnement Ni La. *J Microsc Spectrosc Electron* **10** 291-294.

Pouchou, J.L. & Pichoir, F.M.A. (1988). Determination of mass absorption coefficients for soft x-rays by use of the electron microprobe. In *Microbeam Analysis,* Newbury, D.E. (Ed.) pp. 319-324. San Francisco, CA: San Francisco Press.

Remond, G. Myklebust, R., Fialin, M., Nockolds, C., Phillips, M. & Roques-Carmes, C. (2002). Decomposition of Wavelength Dispersive X-ray Spectra. *J Res Natl Inst Stand* Technol **6** 509-29

Statham, P. & Holland, J. (2014). Prospects for higher spatial resolution quantitative X-ray analysis using transition element L-lines. *IOP Conf Series Mater Sci Eng* **55** 012017

WALDO, R.A. (1988). An iteration procedure to calculate film compositions and thicknesses in electron-probe microanalysis. Microbeam Analysis, 310–314.